



Acoustic characterization of a multi-cavity muffler for broadband noise reduction in flow duct applications

Romain Maréchal, Emmanuel Perrey-Debain, Jean-Michel Ville, Boureima Ouédraogo
Sorbonne Universités, Université de Technologie de Compiègne, Laboratoire Roberval UMR CNRS
7337, CS 60 319, 60 203 Compiègne cedex, France

Summary

In this work, acoustic performances of a novel liner concept based on perforated screens backed by air cavities are investigated both numerically and experimentally for circular ducts with mean flow. Dimensions of the cavity are chosen to be of the order or bigger than the wavelength so acoustic waves within the liner can propagate parallel to the duct surface. In this case the liner becomes non-locally reacting and this gives rise to additional resonance effects which renders the attenuation more effective over a broader frequency range. This work emanates from the Cleansky European HEXENOR project which aim is to identify the best multicavity mufflers configuration for reduction of exhaust noise from helicopter turboshaft engines. In order to predict the mufflers' acoustic performances, a special boundary integral method is presented. Using a tailored Green's function for hard wall circular ducts containing uniform mean flow, the numerical technique only requires the discretization of the perforate screen separating the central channel from the air cavities. Comparisons with experimental measurements are shown in the no-flow case. Flow effects on acoustic performances are shown.

PACS no. 43.55.Rg

1. Introduction

Because exhaust noise from helicopter turboshaft engines [1] still needs an increased attenuation, the HEXENOR project (Helicopter EXhaust Engine NOise Reduction) supported by Cleansky European program, focused on the development and manufacturing of a muffler to be mounted on a turbo-shaft engine exhaust duct. The specifications provided by the Helicopter manufacturer Turbomeca which in addition to be compatible with the exhaust engine design, require to find a good compromise between sound reduction performance, weight and cost constraints. The liner concept based on perforated screens backed by air cavities was therefore selected. This type of liner is commonly used in inlet aircraft engines for which perforated plates are backed with small cavities (honeycomb-like structures). These locally reacting liners have narrow peaks of absorption around the liner resonant frequency [2]. To extend the absorption bandwidth, double or triple layer structures locally reacting liners can be used [3], but this has the consequence of increasing the muffler volume and weight

which may cause substantial departures from the original specifications.

One way of making broadband liners is to enlarge air cavities so that sound propagates not only in the direction normal to the liner but also along the transverse directions. This gives rise to additional resonant effects producing more attenuation over a broader frequency range. The idea of partition spacing in the air backing is discussed in the standard textbook of Ingard [4]. The concept was pushed further by Jing *et al.* [5] for sound propagation in rectangular ducts with mean flow and was also investigated by Allam *et al.* [6, 7] for circular ducts lined with micro-perforated panels (MPP) backed by annular air cavities. In all above-mentioned references, the analysis is restricted to the plane wave mode only. In these circumstances, some of the physical mechanisms involved can be described and anticipated by analyzing the resonance frequencies of the liner sub-cavities as in [5]. In the context of the present work, the broadband nature of combustion noise [1] and the exhaust duct dimensions imply that the frequency range of interest typically lies within the interval $ka \in [0, 5]$ (k is the wavenumber and a is the duct radius) so the muffler necessarily operates in multimodal propagation conditions.

Figure 1 shows a picture of the multi-cavity muffler used for our experimental campaign. The muffler

(c) European Acoustics Association

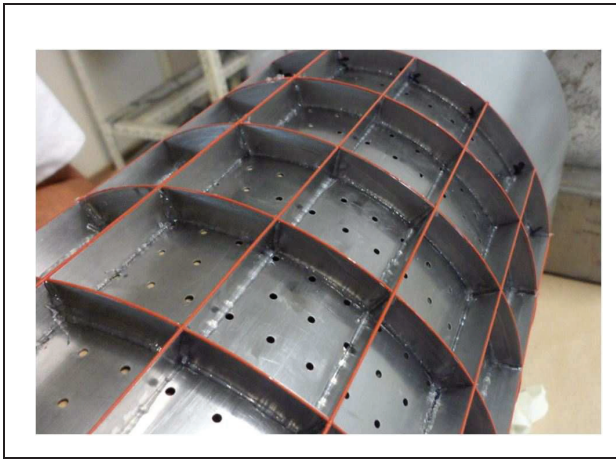


Figure 1. Experimental barrel showing the cavities.

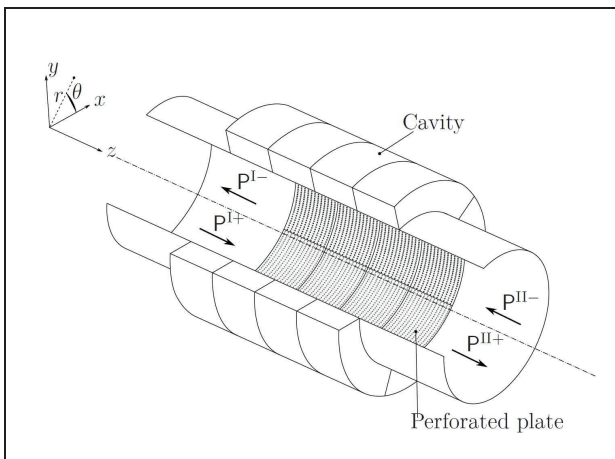


Figure 2. Circular multi-cavity muffler.

which was designed and manufactured by the French Company ATECA, is composed of a 0.5 m long duct with diameter $2a=15$ cm. Cavities size can be varied thanks to 9 removable disks separating the axial cavities and 16 'combs' separating the angular cavities. The plate separating the cavities from the central channel is perforated by laser drilling. The geometrical characteristics of the liner are the cavity depth $h = 10$ mm, the plate thickness $t = 0.5$ mm, the hole diameter $d = 1.89$ mm and the perforation rate $\sigma = 2.51\%$. The methodology used in this paper is based on the determination of the scattering matrix of the muffler using both numerical and experimental approaches. Numerical computations are carried out via integral representation for the acoustic potential whereas experimental measurements are conducted on an acoustic test bench developed during the European project DUCAT [8].

2. Determination of the scattering matrix

The theory starts by expressing the acoustic pressure in the rigid duct regions I and II (see Figure 2) in terms of circular modes, i.e.

$$p(r, \theta, z, t) = \sum'_{m,n} P_{mn}(z) \Psi_{mn}(r, \theta) e^{-i\omega t} \quad (1)$$

where symbol ' signifies that only propagating modes are retained in the summation. Here, normalized modes are explicitly given by

$$\Psi_{mn}(r, \theta) = N_{mn} J_m(\zeta_{mn} r) e^{im\theta}, \quad (2)$$

where N_{mn} is a normalization factor [9], J_m is the Bessel function of the first kind of order m and χ_{mn} is the n^{th} root satisfying the hard wall boundary condition: $J'_m(\zeta_{mn} a) = 0$. Integers m and n denote respectively the angular and radial orders of the duct modes and $P_{mn}(z)$ is the associated modal coefficient. These coefficients combine pressure waves traveling in both positive (+) and negative (-) z directions, so we can write $P_{mn}(z) = P_{mn}^+(z) + P_{mn}^-(z)$. By construction, we have $P_{mn}^\pm(z) = P_{mn}^\pm(0) e^{ik_{mn}^\pm z}$ where

$$k_{mn}^\pm = \frac{-kM \pm \kappa_{mn}}{1 - M^2}, \quad \kappa_{mn} = \sqrt{k^2 - (1 - M^2)\zeta_{mn}^2}$$

is the axial wavenumber for mode (m, n) , $k = \omega/c$ where c is the sound speed and $M = U/c$ is the Mach number. The incoming and outgoing sound pressure vectors are defined with respect to the left and right rigid duct sections z_L and z_R . They contain the value of modal coefficients at the left and right locations. For instance $\mathbf{P}^{I+} = \langle \dots, P_{mn}^{I+}(z_L), \dots \rangle$ etc. where m and n correspond to all propagating modes. The multimodal scattering matrix is defined as the linear relationship between incoming and outgoing sound pressure vectors and

$$\begin{pmatrix} \mathbf{P}^{I-} \\ \mathbf{P}^{II+} \end{pmatrix} = \begin{pmatrix} \mathcal{S}^{11} & \mathcal{S}^{12} \\ \mathcal{S}^{21} & \mathcal{S}^{22} \end{pmatrix} \begin{pmatrix} \mathbf{P}^{I+} \\ \mathbf{P}^{II-} \end{pmatrix}. \quad (3)$$

The procedure to measure the scattering matrix (with no flow) has been published elsewhere [10] and this is briefly reminded here. The acoustic source is driven with a white noise signal in the frequency range 0–3800 Hz which means that the adimensional wavenumber ka remains below 5.3 and the number of propagating modes never exceeds $N = 8$ modes. The acoustic pressure field is measured at 240 points over the cross-section which corresponds to 15 radial positions and 16 angular positions evenly spaced by 22.5° . A modal decomposition is carried out using the Fourier-Lommel transform which yields the complex modal coefficients $P_{mn}(z)$.

The numerical model is based on the integral representation for the acoustic velocity potential φ taking

into account the continuity of normal acoustic displacement (the Myers boundary condition) across the perforate plate:

$$\varphi = \varphi^i + \sum_{j=1}^J \int_{\Gamma_j} \frac{\rho \tilde{Y}}{i\omega} \left(\frac{D\varphi}{Dt} + i\omega\varphi_j \right) \frac{D^*G}{Dt} d\Gamma \quad (4)$$

where G is the duct Green's function satisfying the hard wall condition:

$$G = \sum_{m,n} \frac{\Psi_{mn}(r, \theta) \Psi_{mn}^*(r_0, \theta_0)}{2i\kappa_{mn}} e^{i\psi_{mn}(z-z_0)} \quad (5)$$

with $\psi_{mn}(z) = \frac{-kMz + \kappa_{mn}|z|}{1-M^2}$ and $D/Dt \equiv -i\omega + U\partial/\partial z$ stands for the convective derivative with flow velocity U and φ^i is a given incident field. Here, ω is the angular frequency, ρ the density and where \tilde{Y} is the plate acoustic admittance which is zero at the edges of Γ_j and 1 everywhere except in the close vicinity of the edges (this regularization procedure permits to avoid singular behavior at the junction with the rigid part of the duct [11]). In (4), we consider the partition into J cavities where it is understood that the facing perforate plate Γ_j separates the cavity Ω_j from the main duct. To simplify the analysis the cavities are all identical with rectangle-like shapes in θ and in z . By application of Green's theorem, the potential φ_j in the cavity also satisfies an integral equation:

$$\varphi_j = - \int_{\Gamma_j} G_j \partial_n \varphi_j d\Gamma, \quad (6)$$

where G_j stands for the Green's function associated with the cavity with rigid walls. After discretization of Eqs. (4) and (6), scattering matrix coefficients for the acoustic pressure are obtained using the linearized Euler equation: $p = \rho D\varphi/Dt$.

The transmission loss (TL) is defined as

$$TL = 10 \log_{10} \frac{W^{I+}}{W^{II+}} = 10 \log_{10} \frac{\sum' W_{mn}^{I+}}{\sum' W_{mn}^{II+}}, \quad (7)$$

where $W_{mn} = D_{mn}|P_{mn}|^2$ and modal sound power coefficients are given explicitly by Joseph *et al.* [12].

3. Comparison between experimental and numerical results

We consider first the configuration comprising $N_\theta \times N_z = 8 \times 16 = 128$ cavities (these values correspond to the partitioning with respect to the azimuthal (θ) and axial (z) direction). This configuration behaves as a locally reacting liner with a wall impedance

$$Z^{\text{wall}} = Z_p - i \cot(kh),$$

and best attenuation is expected when the imaginary part of Z^{wall} is zero. Here, the plate impedance model of Allam *et al.* [6] is used in our calculations. The

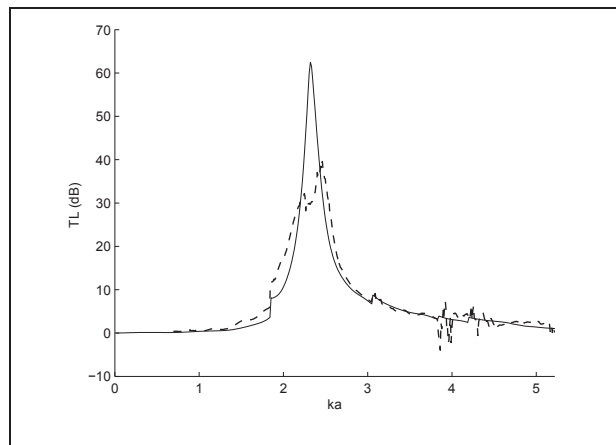


Figure 3. Transmission Loss for the locally reacting liner. Computed (straight line) and measured (dashed line).

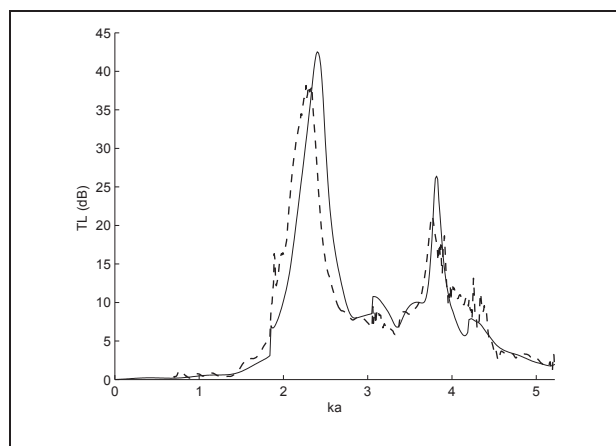


Figure 4. Transmission Loss for the muffler configuration comprising $N_\theta \times N_z = 4 \times 4 = 16$ cavities. Computed (straight line) and measured (dashed line).

sound TL illustrated in Fig. 3 assuming an equi-power modal distribution with random phases which characterizes the combustion noise. Results are in good agreements showing a TL peak near the resonance at $ka = 2.32$ and this value corresponds exactly to the liner resonant frequency. The 20 dB discrepancy between measurements and the calculation are thought to be due to some lack of precision when measuring highly attenuated pressure levels. The presence of a unique peak is typical of SDOF locally reacting liners. The muffler configuration comprising $N_\theta \times N_z = 4 \times 4 = 16$ cavities is now investigated. In the first part of the spectrum, transmission losses of Fig. 4 show similar trends as in Fig. 3 and from $ka \approx 3.5$, a secondary peak emerges showing a maximum attenuation at $ka \approx 3.8$. A closer analysis reveals that this corresponds to the cut-off frequency for the first radial mode (m, n) = (0, 1). Two small peaks can also be identified (especially from the computed results) which correspond to the cut-off frequencies for azimuthal modes ($\pm 2, 0$) and ($\pm 3, 0$).

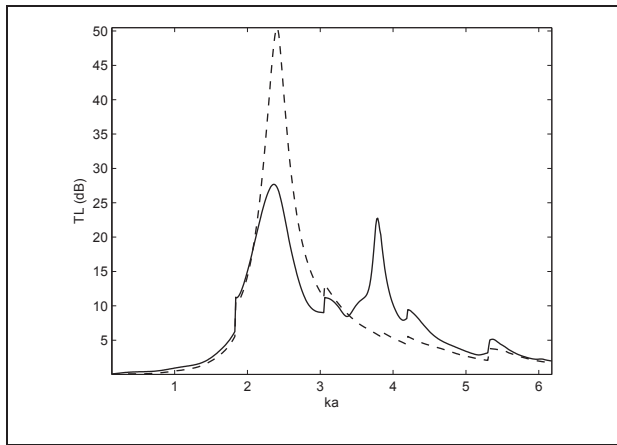


Figure 5. Computed Transmission Loss for the locally reacting liner (dashed line) and the 4×4 configuration (straight), $M = 0.05$.

4. Flow effects

The presence of a flow in the central airway modifies the plate impedance as well as the Myers conditions across the plate (this is taken into account by the convective derivative in the integral equation (4)). According to Allam *et al.* [6], the increase in the normalized resistive part is proportional to M/σ whereas the reactive part slightly decreases. In the case of a locally reacting liner, acoustic performances of Figs. 5 and 6 show a shift of the resonant frequency of the liner (around $ka \approx 3$ when $M = 0.1$) as well as a broadening of the absorption spectrum, this fact was also observed and discussed in [2] for the plane wave mode. These results are compared with the 4×4 configuration. Here again, the presence of resonant cavities gives rise to other TL peaks corresponding to the cut-off frequencies for azimuthal modes $(\pm 2, 0)$ for $M = 0.05$ and $(\pm 3, 0)$ for $M = 0.1$. The drawback is a degradation of performances around the locally reacting liner resonant frequency. When $M = 0.2$, our calculations in Fig. 7 show that additional resonant and scattering effects expected from the 4×4 configuration are somewhat smoothed out by the presence of the flow and classical locally reacting linings provide the best attenuation.

5. Conclusions

Sound propagation through a circular multi-cavity muffler has been analyzed both numerically and experimentally via the determination of the scattering matrix. The measurement procedure allows to consider multimodal propagation conditions up to the non-dimensional frequency $ka = 5.3$ which corresponds to 8 propagating modes. Scattering matrix coefficients are computed via an integral representation for the acoustic velocity potential in circular ducts with uniform flow. In the no-flow case, both mea-

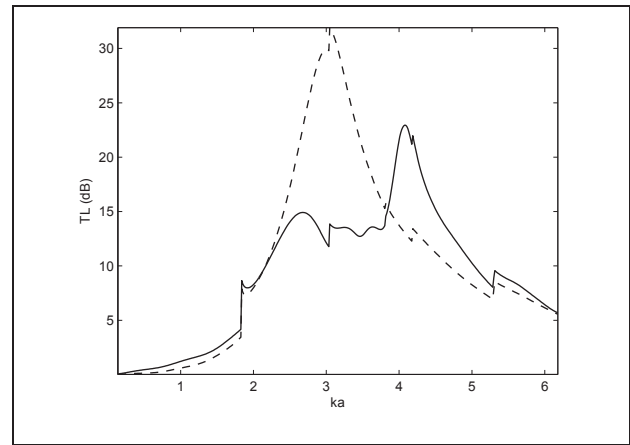


Figure 6. Computed Transmission Loss for the locally reacting liner (dashed line) and the 4×4 configuration (straight), $M = 0.1$.

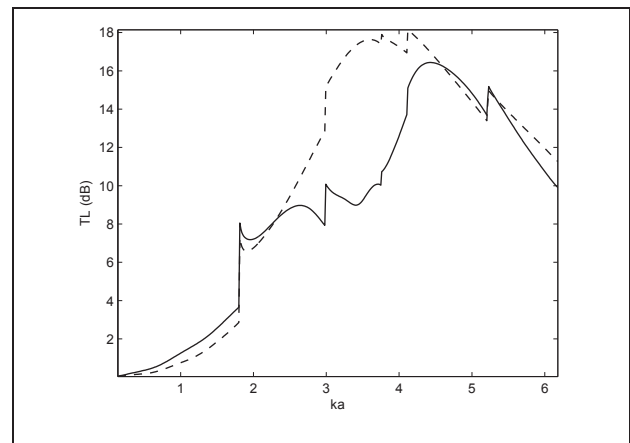


Figure 7. Computed Transmission Loss for the locally reacting liner (dashed line) and the 4×4 configuration (straight), $M = 0.2$.

sured and computed results are found to be in good agreement and the presence of large cavities behind the perforate plate gives rise to additional resonant and scattering effects which broadens the absorption bandwidth. However the presence of the flow in the central airway tend to smooth out these effects and this may render the multi-cavity muffler less efficient than standard locally reacting liners. Of course, these conclusions are valid for the particular case treated here and the benefit of the multiple-cavity resonance lining largely depends on the duct and cavities dimensions as well as the nature of the incident field.

Acknowledgement

This work is part of the European project HEXENOR part of the Clean Sky program. Thanks to Turbomeca for his contribution to the project.

References

- [1] I. Duran, S. Moreau, F. Nicoud, T. Livebardon, E. Bouty, T. Poinso: Combustion noise in modern aero-engines. *Aerospace Lab Journal* 7 (2014) 1–11.
- [2] M. Namba, K. Fukushige: Application of the equivalent surface source method to the acoustics of duct systems with non-uniform wall impedance. *Journal of Sound and Vibration* 73 (1980) 125–146.
- [3] S.S. Jung, Y.T. Kim, D.H. Lee, H.C. Kim, S.I. Cho, J.K. Lee: Sound absorption of micro-perforated panel. *Journal of the Korean Physical Society* 50 (2007) 1044–1051.
- [4] U. Ingard: *Noise reduction analysis*. Jones and Bartlett Publishers, 2010.
- [5] X. Jing, X. Wang, X. Sun: Broadband acoustic liner based on the mechanism of multiple cavity resonance. 13th AIAA/CEAS Aeroacoustics Conference (28th AIAA Aeroacoustics Conference) 2007, paper 3527.
- [6] S. Allam, M. Abom: A new type of muffler based on micro-perforated tubes. *Journal of Vibration and Acoustics* 133 (2011).
- [7] S. Allam, M. Abom: On optimal design of mufflers using micro-perforated panels. *The 17th International Congress on Sound and Vibration* 2010.
- [8] E.R. Rademaker: Publishable synthesis report DUCAT. Report DUCAT-NL-01-T5-9, 2001
- [9] E. Perrey-Debain, R. Maréchal, J.-M. Ville: Side-branch resonators modelling with Green's function methods. *Journal of Sound and Vibration* 333 (2014) 4458–4472.
- [10] M. Taktak, J.-M. Ville, M. Haddar, G. Gabard, F. Foucart: An indirect method for the characterization of locally reacting liners. *J. Acoust. Soc. Am.* 127 (2010) 3548–3559.
- [11] E. Luneville, J.-F. Mercier: Mathematical modelling of time-harmonic aeroacoustics with a generalized impedance boundary condition. *Mathematical Modelling and Numerical Analysis* 48 (2014) 1529–1555 .
- [12] P. Joseph, C.L. Morfey, C.R. Lewis: Multi-mode sound transmission in ducts with flow. *Journal of Sound and Vibration* 264 (2003) 523–544.